Thermochimica Acta, 51 (1981) 45—52
Elsevier Scientific Publishing Company, Amsterdam — Printed in The Netherlands

VACUUM BALANCE STUDIES OF MILLED MATERIAL AND MECHANOCHEMICAL REACTIONS

D.R. GLASSON
John Graymore Chemistry Laboratories, Department of Environmental Sciences,
Plymouth Polytechnic, Plymouth, PL4 8AA, Devon, England

ABSTRACT

The types of change in surface properties and porosity of milled materials having widely different hardness and crystal structure are reviewed. For more intensive milling, the use of vacuum balance techniques in conjunction with X-ray diffraction, optical- and electron-microscopy enables changes in microstructure and phase composition to be determined during mechanochemical reactions.

Metallic or non-metallic harder materials (Mohs scale 8-9), such as transition metal nitrides or silicon nitride and boron carbide, increase their surface on milling largely due to brittle fracture, so that the surface area tends towards an upper limiting value with comparatively little development of porosity.

Softer materials (Mohs scale 1-2), such as gypsum, china clay(Kaolinite) and hydrated lime and magnesia undergo plastic deformation and strain hardening on longer milling, so that the surface area passes through a maximum before decreasing to an equilibrium value. This is applicable also to materials of intermediate hardness (Mohs scale 3-5), such as calcite, magnesite and dolomite, provided that the milling is sufficiently intensive; the flow and welding processes during the plastic deformation leave the grains non-porous to nitrogen gas, but adsorption of water vapour causes development of porosity, a phenomenon also observed with lunar fines (mainly silicate minerals) which are of somewhat greater hardness but contain amorphous surface layers (cf. Beilby layer) and nuclear particle damage tracks having tubular pores with narrow constrictions forming micropores.

More intensive milling can result in crystal transformations and mechanochemical reactions. Thus gypsum is converted to anhydrite, viz., $CaSO_4.2H_2O \rightarrow CaSO_4.\frac{1}{2}H_2O \rightarrow \gamma\text{-}CaSO_4 \rightarrow \beta\text{-}CaSO_4$. Calcite, $CaCO_3$, is converted to aragonite, while calcitic $CaCO_3$ and magnesite, $MgCO_3$, form dolomite $CaCO_3.MgCO_3$.

INTRODUCTION

Milling of solids usually enhances reactivity by increasing the surface area and number of crystallites and producing crystal strain. For harder materials, these changes are largely due to brittle fracture, so that the surface area increases to an upper limiting value with comparatively little development of porosity. Softer materials undergo plastic deformation and strain hardening on longer milling, so that the surface area subsequently decreases to an equilibrium value. Materials of intermediate hardness behave similarly on sufficiently intensive milling, with the flow and welding processes during the plastic deformation reducing porosity. Phase transformations and mechanochemical reactions (1-6) can result from more intensive milling, where critical amounts of crystal lattice distortion of about 1-2% have been developed. Recovery of crystallinity in samples severely disordered by milling is possible by thermal treatment(7).

Changes in microstructure and phase composition may be determined by vacuum balance techniques (for measuring surface area and porosity by gravimetric B.E.T. gas sorption(8)) used in conjunction with X-ray diffraction (for phase identification and strain from X-ray line- (or peak-) broadening), optical- and electron-microscopy (for crystallite and aggregate sizes).

EXPERIMENTAL TECHNIQUES

Milling of materials

The harder materials (Mohs scale 8-9), such as transition metal nitrides or silicon nitride and boron carbide, were milled in a vibration mill (Glen Creston) using tungsten carbide ball pestles. Softer materials (Mohs scale 1-2), such as gypsum, china clay (Kaolinite) and hydrated lime and magnesia were milled in ball-mills containing porcelain balls or in small roller mills containing cylindrical agates. Materials of intermediate hardness (Mohs scale 3-5) such as calcite, magnesite and dolomite were milled in ball-mills containing porcelain or stainless steel balls. The latter were found more satisfactory; the brittle enstatite porcelain ($MgSiO_3$) balls wore at a rate about 250 times faster than those of the ductile steel(9). Thus small charges of 15 g were intensively steel-ball milled with the pot filled to 50% volume with steel balls and the charge only sufficient to form a thin film of about 10 $mgcm^{-2}$ on the interior surface of the mill. There were only small and practically steady rates of iron uptake by the charges of about 4-10 ppm per hour (analysis by atomic absorption spectroscopy, after dissolving portions of the samples in hydrochloric acid).

Examination of the samples

Phase composition and apparent crystal strain were determined from X-ray diffraction patterns and line- (or peak-) broadening, after allowing for any effects due to very small crystallite size (below 0.1 μm). The surface areas were determined by a gravimetric B.E.T. method(8), using nitrogen (or occasionally oxygen) gas sorption at -183° or -196°C recorded on an electrical sorption balance(10) (quarter mg sensitivity using 5-10 g samples) or on vacuum microbalances (μg to mg sensitivity using 0.25 g samples or less), viz., Sartorius or CI Microforce Mark 2B. The adsorption isotherms also indicated any porosity present (from hysteresis) and pore size ranges. Average crystallite sizes deduced from the specific surfaces of the less porous materials were compared with aggregate sizes observed by optical- and electron-microscopy (Philips TEM 300 or Jeol SEM 35).

RESULTS AND DISCUSSION

Harder materials

Metallic or non-metallic harder materials (Mohs scale 8-9), such as transition metal nitrides(11), silicon nitride or boride(12) and boron carbide(13), develop surface on milling largely due to brittle fracture. This is illustrated in Fig. 1(a), where the surface area of titanium nitride increases towards an upper limiting value as milling proceeds(11). The high temperatures required for producing refractory hard metals cause sintering to the extent that samples generally have sp. surfaces of below 1 m^2g^{-1} and average crystallite sizes (equivalent spherical diameters) of over 2 μm. Since the adsorption isotherms show practically no hysteresis, the absence of porosity permits the average crystallite sizes to be determined from the surface areas, cf. Fig. 1(b). Accordingly, electron-micrographs showed that the original nitride consisted of single crystals and aggregates of about 0.5-5 μm size. The single crystals were fractured during the earlier stages of the milling and the fragments were incorporated into the aggregates which remained approximately the same size throughout the milling. Thus the average crystallite size decreased rapidly at first and later slowly when the crystallites became of submicron size. When aggregation and attrition proceed at equal rates, a "grinding equilibrium" is established and the specific surface and average crystallite size remain practically constant. Hence most of the crystal strain, η, (in Fig. 1(c)) developed during the first 2 h milling and subsequently remained practically constant. Other transition metal nitrides showed similar behaviour on milling. Also in a sample of tantalum nitride containing about equal parts of ε-$TaN_{0.9-1.0}$ and δ-$TaN_{0.8-0.9}$ (overall $TaN_{0.93\pm0.03}$ from analysis), the ε-form progressively converted to the δ-form during 10 h milling. The crystal lattice transformation from a hexagonal CoSn(B_{35}) to WC(B_n)-type lattice involves an increase of about 2% in the <u>a</u>-dimensions within the layers and a decrease of about 1% in the <u>c</u>-distance between the layers. Since the true homogeneity range of the ε-TaN is nearer 1 than 0.9 atom N per Ta (0.99-1.00) and that of the δ-structure is nearer 0.9

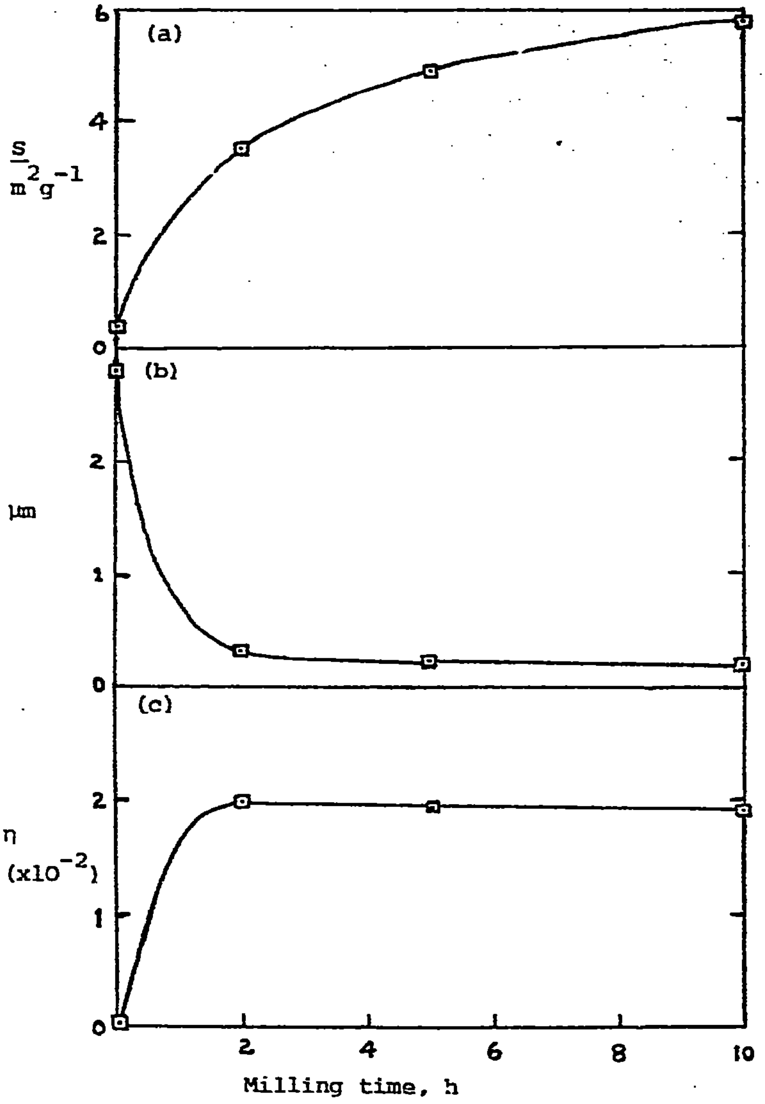

Fig. 1. Milling of Titanium Nitride.

than 0.8 (0.87–0.90), the crystal lattice transformation evidently adjusts the distribution of nitrogen to approach these homogeneity ranges favourable to the δ- and ε-structures.

Softer materials

Materials (Mohs scale 1–2) such as gypsum, china clay or hydrated lime and magnesia undergo plastic deformation and strain hardening on longer milling, so that the surface area passes through a maximum before decreasing to an equilibrium value when disintegration and re-aggregation proceed at the same rates.

This is illustrated in Fig. 2 for hydrated lime, where ball milling using porcelain balls of assorted sizes instead of equal sizes produced a more rapid increase in surface, but subsequently there is loss of surface when the crystallites aggregate. This is found also in the milling with cylindrical agates and is analogous to the behaviour of magnesium hydroxide on ball milling(14). The anisotropy of the $Ca(OH)_2$ and $Mg(OH)_2$ crystal lattices (hexagonal layer structures) tends to cause the original crystallites to fracture into layers which shear(tear) to some extent, before aggregating by stacking which ultimately causes the surface area to effectively decrease somewhat. A similar loss of surface has been found in the longer milling of kaolin(15). During the changes, the materials show a limited porosity, indicated by a small adsorption hysteresis to nitrogen. Longer milling (beyond 5h) introduces appreciable strain into the materials, especially during ball milling where the impaction is greater than in the rotary milling action of the cylindrical agates, which produces mainly shear, cf. extent of X-ray line-broadening. These differences in milling action also lead to differences in shapes of aggregates, cf. electron-micrographs, as reflected in variations in the rheological properties of hydrated lime suspensions and putties. Thermogravimetric behaviour is also modified(16).

Fig. 2 $Ca(OH)_2$ Fig. 3 $CaCO_3$

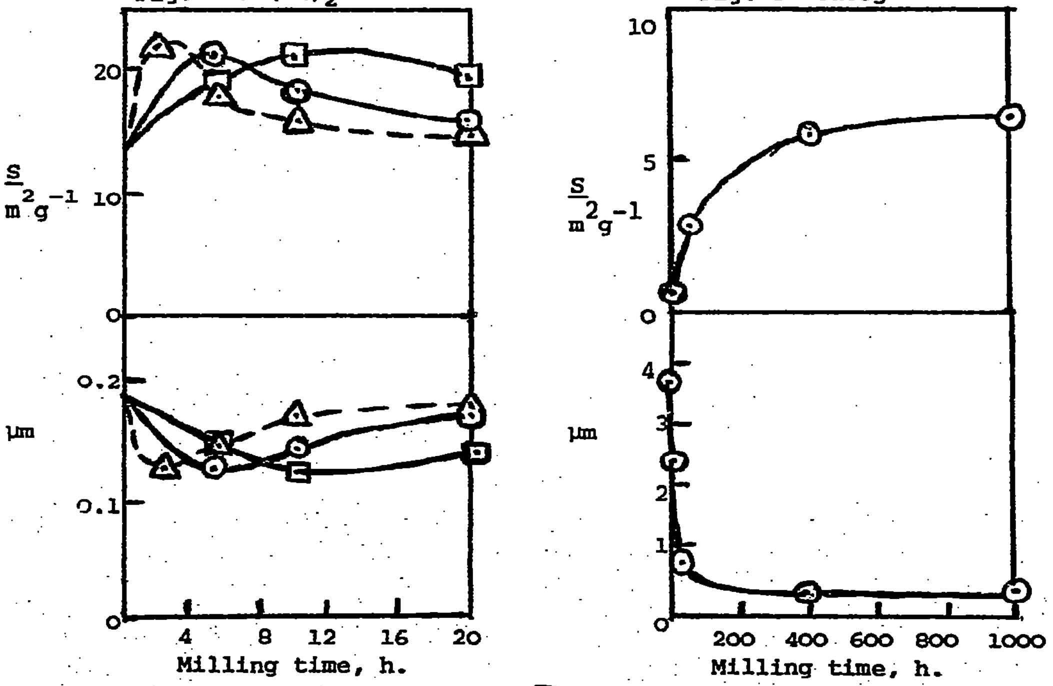

Key to Fig. 2; Ball-milled ⊡ equal sizes, ⊙ assorted sizes, △ Cylindrical agates

Fig. 2 and 3 Surface areas and average crystallite sizes of ground $Ca(OH)_2$ and $CaCO_3$ samples

Milling of gypsum results in an increase of surface from 1.4 to 4.2 m^2g^{-1} while it dehydrates to $CaSO_4$, $\frac{1}{2}H_2O$, from $CaSO_4$, $2H_2O$. There is subsequent loss of surface as the $CaSO_4$, $\frac{1}{2}H_2O$ dehydrates to γ-$CaSO_4$ (which has approximately the same layer lattice with water removed), before conversion and densification (2.45 to 2.96) to β-$CaSO_4$, anhydrite.

Materials of intermediate hardness

Calcite, magnesite and dolomite (Mohs hardness 3-5) are not laminar materials like china clay, or hydrated lime and magnesia which show easy cleavage. Thus with moderately intense milling conditions, calcite (Iceland Spar) behaves similarly to the harder materials, cf. Fig. 3 with Fig. 1. However, under high confining pressure and/or temperature calcite crystals flow plastically on a multiple slip system. Hence during ball milling, the processes of flow and plastic deformation leave the grains non-porous to adsorbed nitrogen, but adsorption of water vapour causes development of porosity, a phenomenon also observed with lunar fines (mainly silicate minerals) which are of somewhat greater hardness but contain amorphous surface layers (cf. Beilby layer) and nuclear particle damage tracks having tubular pores with narrow constrictions forming micropores. The pore system in the ground calcite is more open, the capillary condensation behaviour suggesting the presence of slit-shaped openings of width about 36 A.(17).

The grinding of small quantities of either calcite, aragonite or vaterite in a stainless steel ball mill produces phase transformations,(3). In each instance the end product is an equilibrium mixture of calcite and aragonite. Before the phase transformation calcite to aragonite can occur, a critical amount of lattice distortion, about 1.5%, must be developed. The calcite produced from transforming aragonite appears with and maintains the same distorted lattice. Vaterite is very unstable in the mill and transforms rapidly, first to calcite and then to a calcite-aragonite mixture. Each crystalline form of calcium carbonate is deformed plastically, and in a flowing together and apart of the grains a grinding equilibrium is established with an equivalent particle size of about 860 nm. The precipitated calcite suffered a marked reduction in specific surface from 20.3 to 3.2 m^2g^{-1}, while vateritic $CaCO_3$ decreased from 5.8 to 2.6 m^2g^{-1} and the aragonitic $CaCO_3$ increased slightly from 2.3 to 2.5 m^2g^{-1}. The changes for the calcitic $CaCO_3$ are shown in Fig. 4.

The above milling was found later to be sufficiently intensive for a sample of magnesite ($\underline{S}$ = 0.6 m^2g^{-1}, average crystallite size, 3.3 μm) to reach a maximum specific surface of 12.3 m^2g^{-1} before decreasing to about 4 m^2g^{-1} (Fig. 4). Similar changes were shown on milling dolomite. When the precipitated calcite was milled with a stoicheiometric amount of the magnesite (1:1 molecular ratio), the specific surface of the mixture progressively decreased. Some of

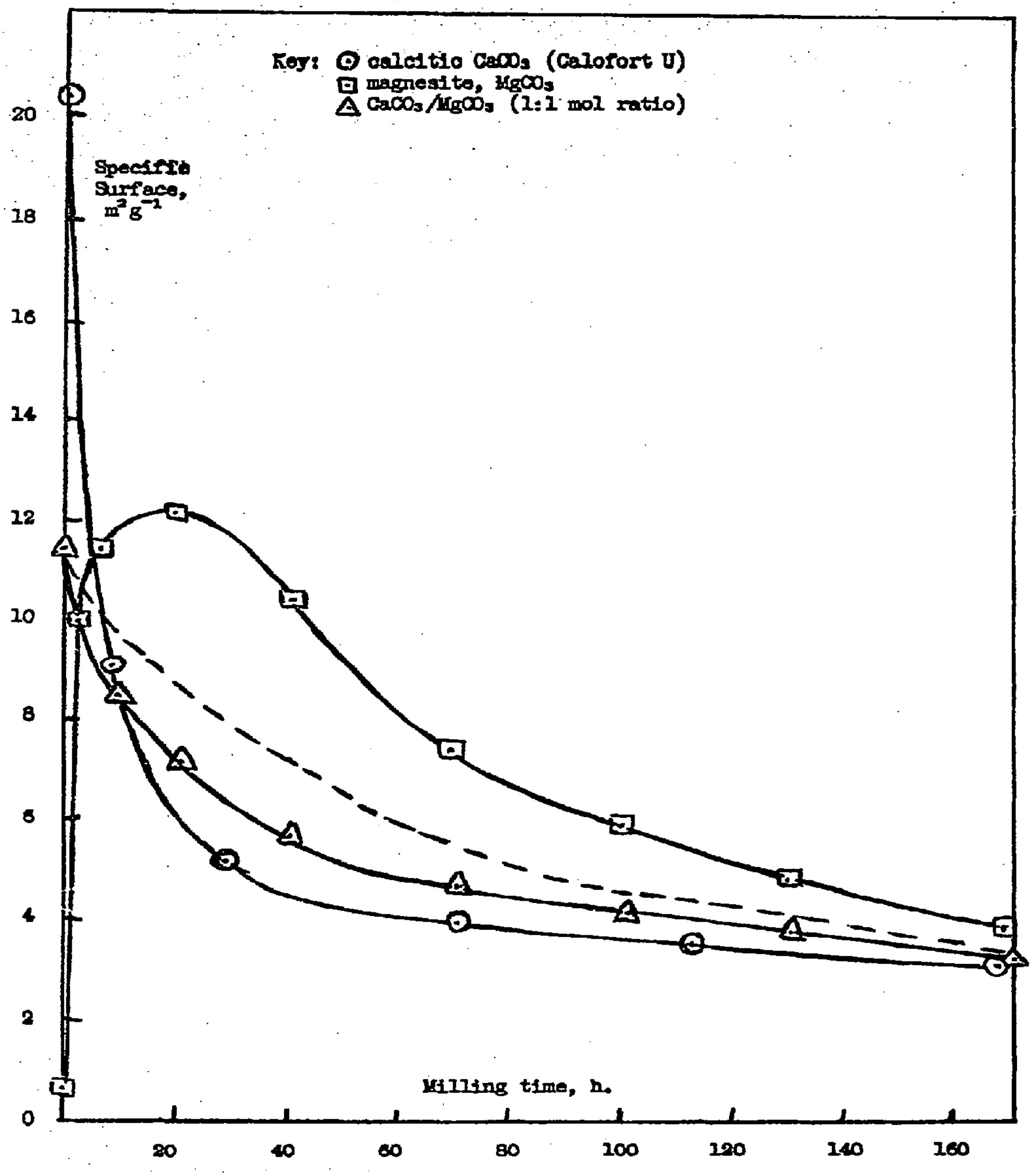

Fig. 4. Milling of calcitic $CaCO_3$, magnesite and mixed $CaCO_3/MgCO_3$ (1:1 mol ratio)

the calcite was converted to aragonite, while the remainder incorporated magnesite into its crystal lattice to produce dolomite. Formation of the dolomite was found to ease crystal strain (from X-ray line- (or peak-) broadening) and also caused decrease in surface, since the experimental curve for the $CaCO_3/MgCO_3$ mixture (Fig. 4) is lower than the broken-lined curve representing changes in specific surface if there was not interaction between the components. However, prolonged milling again leads to equilibrium values for the specific surface of about 3 m^2g^{-1}, as found for mineral dolomite after about 200 h milling.

REFERENCES

1 R.B. Gammage and D.R. Glasson, Chemy. Ind., 1963, p.1466
2 D.R. Glasson, Chem. Soc. Internat. Symposium, Aberdeen, July 1966, No. 7, 5 pp
3 R.B. Gammage and D.R. Glasson, J. Colloid Interface Sci., 55(2)(1976)396-401
4 I.J. Lin and S. Nadiv, Mater. Sci. Eng., 39(1979)193-209
5 G. Martinez, J. Morales and G. Munera, J. Colloid Interface Sci., 1981 in press
6 R.B. Gammage, D.R. Glasson, I.R. Hodgson and P. O'Neill, J. Colloid Interface Sci., 1981 in press
7 R.B. Gammage and D.R. Glasson, Colloid and Interface Science, Vol. V, Academic Press, London and New York, 1976, pp. 437-52
8 D.R. Glasson, J. Chem. Soc., 1956, pp. 1506-10
9 R.B. Gammage and D.R. Glasson, J. Colloid Interface Sci., 71(3)(1979)522-5
10 S.J. Gregg, J. Chem. Soc., 1946, pp. 561-3
11 Irshad Ali, D.R. Glasson and S.A.A. Jayaweera, Journées d'Etude sur les Nitrures. II. Limoges, France, April, 1975
12 B. J. Brockington, D.R. Glasson, S.A.A. Jayaweera and J.A. Jones, Journées d'Etude sur les Nitrures. I. Rennes, Brittany, France, May 1973
13 D.R. Glasson and J.A. Jones, British Ceramic Research Association Symposium, Stoke-on-Trent, July 1970
14 S.J. Gregg and J.P. Saenz, J. appl. Chem., Lond., 16(1966)300-4
15 S.J. Gregg, T.W. Parker and M.J. Stephens, J. appl. Chem., Lond., 4(1954)666-71
16 R.B. Gammage, D.R. Glasson and R. Srodzinski, 2nd Anglo-French Symposium on Thermal Analysis (CS-AFCAT), Plymouth, England, September 1977. Proceedings, pp. 97-100.
17 R.B. Gammage, H.F. Holmes, E.L. Fuller Jr., and D.R. Glasson, J. Colloid Interface Sci., 47(2)(1974)350-64.